University of Thi-Qar Journal of Science (UTsci)
The 4th Scientific Conference of Science College/ University of Thi_Qar
Volume (7), No.2

Synthesis and Optical Studies of the 3,4-dimethoxy Benzaldehyde [5-(2-hydroxyphenyl)-1,3,4-oxadiazol-2-yl]Hydrazone Metal Complexes

*Athraa H. Mekkey
Department of Chemistry
College of Science
University of Thi-Qar
Nasiriya, Iraq
*athraa84_chem@sci.utq.edu.iq

Fatima H. Malk
Department of Materials Science
Polymer Research Center
University of Basrah
Basrah, Iraq

Samah H. Kadhim
Department of Chemistry
College of Science
University of Thi-Qar
Nasiriya, Iraq
Samah.h-chem@sci.utq.edu.iq

***Abstract*-The aim of the present study is to synthesize and optical studies of 3,4-dimethoxy benzaldehyde [5-(2-hydroxyphenyl)-1,3,4-oxadiazol-2-yl]hydrazone metal complexes. Firstly, the 3,4-dimethoxybenzaldehyde [5-(2-hydroxyphenyl)-1,3,4-oxadiazol-2-yl] hydra zone was synthesized by the reaction of the 2-(5-hydrazino-1,3,4-oxadiazol-2-yl)phenol with 2,3-dimethoxybenzaldehyde in the ethanol as a solvent . Scondly, its complexes of Cr(III), Fe(III), Co(II) and Ni (II) have been synthesized. The synthesized coumpounds and its metal complexes were characterized by the FTIR, Mass spectra and UV-vis absorption. The results confirmed the suggested square planar geometry of the Ni (II) complex and tetrahedral geometry of the Co(II) complex, while Cr (III), Fe(III) complexes were assigned octahedral geometrics. The optical absorption spectra of those complexes in the wavelength range from 200-900 nm were studied.The results showed that the optical absorption is due to indirect allowed transitions of the compound and its complexes, the energy gap (Eg) of these compounds decreases in the order L> Ni (II)> Fe(III)> Co(II) and > Cr(III), the absorption coefficient (α), real and imaginary parts (ε_r,ε_i), and optical conductivity (σ_{opt})were estimated.**

***Keywords*— Oxadiazole, Optical properties, Energy gap.**

I. INTRODUCTION

One of the most interesting areas of research is the electrically conducting organometallic [Sheats.et al., 1984]. The method of the producing conducting organometallic involves complexion transition metals with conjugated bridging ligands. The ability of the alter the oxidation state of the metal ion and the charge density along the ligand provides an alternative route to charge carrier creation as opposed to redox doping.

Metal complexes containing oxadiazole moiety such as 1,3,4-oxadiazole derivatives have aroused considerable interest in view of their industrial and biological importance [Farhanullah et al., 2004]. Many of these compounds possess a wide spectrum of medicinal properties, including activity against tuberculosis, leprosy, and bacterial and viral infections. It was found that these compounds are active against influenza, protozoa, smallpox, psoriasis, rheumatism, trypanosomiasis, coccidiosis, malaria and certain kinds of tumors and have been suggested as possible pesticides and fungicides. Their activity has frequently been thought to be due to their ability to chelate trace metals [Khan.et al., 1990, Khan.et al., 1991].

Optical properties such as refractive indices for certain range of wavelength between ultraviolet and near infrared and optical band gap values are becoming quite important criteria for selection of application of the fabricated films; the refractive indices of optical materials have considerable importance for applications in integrated optic devices such as switches [Zhu .et al., 2006].

The absorption coefficient near fundamental absorption edge in both of crystalline and amorphous semiconductors is dependent on the photon energy. For direct transitions, the absorption coefficient was taken on the following more general form as a function of photon energy [Hussein.et al.,2014].

$$\alpha h \upsilon = A (\alpha h \upsilon - E g)n \quad (1)$$

And for indirect transition

$$\alpha h \upsilon = B (\alpha h \upsilon - E g)n \quad (2)$$

where υ is the frequency of the incident photon , n is the number which characterizes the optical processes .n has the value 1/2 for the direct allowed transition , 3/2 for a forbidden direct allowed transition and 2 for the indirect allowed transition , A and B are constants and Eg is the optical energy gap. When the straight portion of the graph of $(\alpha h\upsilon)^n$ against hυ is extrapolated to $\alpha = 0$ the intercept gives the transition band gap [Ezema.et al., 2005].

The optical absorption coefficient α (cm-1) which is a function of wavelength can be calculated from the optical absorbance spectra by using the relations [Ezema.et al., 2005].

$$I = I0\ e^{-\alpha t} \quad (3)$$

Where I is the incident intensity and I0 is the penetrating light intensity, and t is the thicknesses of matter (cm) .

The absorption coefficient can be calculated by:

$$\alpha = 2.303(A/t) \quad (4)$$

The refractive index n can be expressed by:

$$n = (1+\sqrt{R})/(1-\sqrt{R}) \quad (5)$$

The extinction coefficient K can be calculated by:

$$k = \alpha\lambda/4\pi \quad mm \quad (6)$$

The real and imaginary complex dielectric constants can be expressed by Equation 7 and 8, respectively:

$$\varepsilon' = n2-k2 \quad (7)$$

$$\varepsilon i = 2nk \quad (8)$$

The optical conductivity, σopt ,is related to light speed and can be expressed by the following equation:

$$\sigma_{opt} = \alpha nc/4\pi \quad (9)$$

The present study discuss the synthesis, characterization and optical conductivity of heterocyclic ligands towards Cr(III), Fe(III), Co(II) and Ni(II) ions .

II. MATERIALS AND METHODS

All chemical compounds were used as received without purification. They were obtained from BDH, Sigma Aldrich and Fluka. All metal salts were used as chlorides.

A. Physical Measurment

The melting point or the decomposition temperature of the prepared ligand and its metal complexes were observed in an electro thermal melting point apparatus model (Melting SMP31). The FTIR spectra were recorded using KBr disc on Shimadzu FTIR spectrophotometer (Model: IR- affinity, Shimadzu) in the rang (250-4000) cm-1. Mass Spectra were obtained using (Network Mass Selective Detector5973). The spectra of absorption were recorded for wavelengths 200-900 nm using UV-visible spectrophotometer model (U-V25400-38) by SHIMADZU Co. Purity of the ligand and its metal complexes were tested by Thin Layer Chromatography (TLC).

B. Preparation of the Ligand

The template is used to format your paper and style the text. All margins, column widths, line spaces, and text fonts are prescribed; please do not alter them. You may note peculiarities. For example, the head margin in this template measures proportionately more than is customary. This measurement and others are deliberate, using specifications that anticipate your paper as one part of the entire proceedings, and not as an independent document. Please do not revise any of the current designations.

1) Synthesis of 3-hydroxybenzohydrazide (A) .

A mixture of methyl 3-hydroxybenzoate (15.2ml, 0.1mol) and hydrazine hydrate (10ml, 0.2mol) was dissolved in (100 ml) ethanol. The mixture was refluxed for 8 hours, then the solvent evaporated to half .The solid product was collected and recrystallized using methanol [Zoulikha.et al.,2007 , Athraa , et al , 2019]. Melting point 148 °C, yield 95%.

2) Synthesis of 3-(5-mercapto-1,3,4-oxadiazol-2-yl)phenol (B)

To 3-hydroxybenzohydrazide (A) (15gm , 0.1mol) and potassium hydroxide (5.6gm , 0.1mol) in absolut ethanol 50ml, carbon disulfide (6ml 0.1mol) in 50ml ethanol was added. The mixture was refluxed until H_2S gas evaporation has been stopped. The solvent was evaporated and the mixture was acidified with HCl (25%) . The solid product formed was filtered, recrystallized from ethanol absolute [Zoulikha.et al., 2007]. The solid (B) had awhite color , melting point 225 °C, yield 80%.

3) Synthesis of 3-(5-hydrazinyl-1,3,4- oxadiazol-2-yl) phenol (C)

Amixtur of 3-(5-mercapto-1,3,4-oxadiazol-2-yl)phenol (B) (6.5gm ,0.028 mol) and hydrazine hydrate (1.8ml ,0.057 mol) in ethanol (50 ml) was heated for 20 hours. Then the mixture was concentred and then cooled [Saddam,.et al , 2017., Samah , 2012] The solid particles were filtered and the crude product recrystallized from ethanol. The prepared crystals had a melting point of 222 °C, yield 61.5%.

4) Synthesis of Compound 3-(5-(2-(2,3-dimethoxybenzylidene)hydrazinyl) 1,3,4-oxadiazol-2-yl]phenol (L1)

The 3-(5-(2-(2,3-dimethoxybenzylidene)hydrazinyl) 1,3,4-oxadiazol-2-yl]phenol(D) was synthesized by acondensation reaction of the 3-(5-hydrazino-1,3,4-oxadiazol-2-yl) phenol (C) with dimethoxybenzaldehyde (1.92gm ,0.01mol) (1.66 gm, 0.01mol) in ethanol (50 ml) was refluxed for 4 hours. The solid product formed was filtered with a glass funnel, then recrystallized from ethanol to get a yellow ligand , yield 80%. Figure (1) shows the prepared materials. [Athraa.et al , 2019 ., Wathiq.et al., 2012 ، Athraa.et al., 2012]

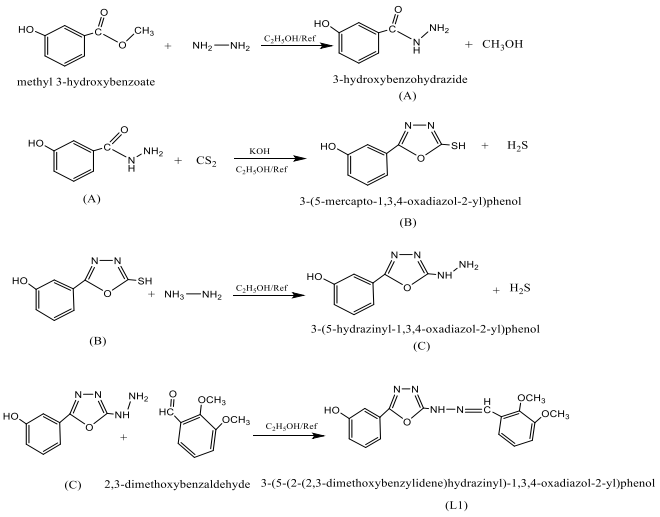

Fig. 1. Synthesis of ligand

C. *Preparation of Complexes*

The complexes were synthesized by mix (0.001mol) from ligand L1 with salts (0.001mol) from salts [$CrCl_3.6H_2O$, $FeCl_3.6H_2O$, $CoCl_2.6H_2O$ and $NiCl_2.6H_2$] both alone in (50ml) ethanol and refluxed for 3 hours (monitored by TLC) .Then the precipitate was filtered and washed with ethanol or aqueous ethanol to remov unreacted salts or ligand ,afterwareds the precipitated complexes were dried [Ibrahim.et al., 2012]

III. RESULTS AND DISCUSSION

A. *FT-IR Spectra*

The main FTIR data of the ligand L1 and its complexes are summarized in Table (1). The free ligand exhibited six major bands at (3525) cm^{-1}, (3218) cm^{-1}, (1614) cm^{-1},(1536) cm^{-1}, (1245) cm^{-1} and (1338) cm^{-1} which refer to the following stretching vibration (υ OH), (υ NH_2), (υ C=N) imine [Redha.et al.,2014 , Dharkar , .et al.,2011 ,ٔAthraa .et al.,2015], (υ C=N) oxa, (υ C-O-C) sym and (υ C-O-C) asy respectively. As shown below (Table 1). In the metal complexes new bands were formed attributed to the coordinated (M-N), (M-O) and (M-Cl) bonds and appeared at the region (462-532) cm^{-1}, (354-378) cm^{-1} and (208-270) cm^{-1} respectively. This indicates that the coordinate occurred through the (N), (O) and (Cl) atoms.

TABLE 1. IR Frequencies (cm-1) of the Compound and their Metal Complees

Compound	(OH)	(NH)	imine(C=N)	υ(C=N)	(C–O–C)	(M–N)	(M–O)	(M–Cl)
$C_{17}H_{16}N_4O_4$	3525	3218	1614	1536	1338 (Asy) 1245(sy)	---	---	---
$[Cr(L_1)Cl_3]$	3572	3286	1612	1535	1338(Asy) 1242(sy)	516	362	270
$[Fe(L_1)Cl_3]$	3550	3255	1620	1550	1350(Asy) 1244(sy)	532	359	248
$[Co(L_1)Cl_2]$	3487	3271	1618	1566	1296(Asy) 1240(sy)	520	378	208
$[Ni(L_1)Cl_2]$	3533	3101	1622	1473	1319(Asy) 1232(sy)	462	354	262

B. *Mass Spectra*

The purity of L1, $[Cr(L_1)\ Cl_3]$, $[Fe(L_1)\ Cl_3]$, $[Co(L_1)Cl_2]$ and $[Ni(L_1)Cl_2]$ was checked from mass spectra Figures (2-6), where the spectra showed that a clear base peaks (m/e) molecular weights and the intensity (%).

The mass spectrum of the ligand exhibits a molecular ion peak $[M]^{+\cdot}$ at 340 m/e. The mass spectrum of the complexes $[Cr(L_1)\ Cl_3]$, $[Fe(L_1)\ Cl_3]$, $[Co(L_1)Cl_2]$ and $[Ni(L_1)Cl_2$ shows a molecular ion peak $[M]^{+\cdot}$ at (498), (502) , (465) and (467) which is equivalent to the molecular mass of the complexes respectively.

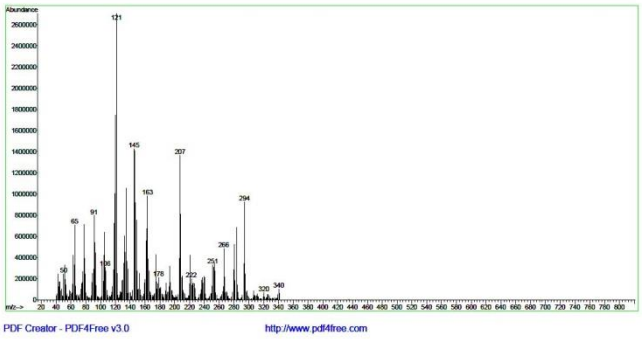

Fig. 2. Mass spectra of ligand

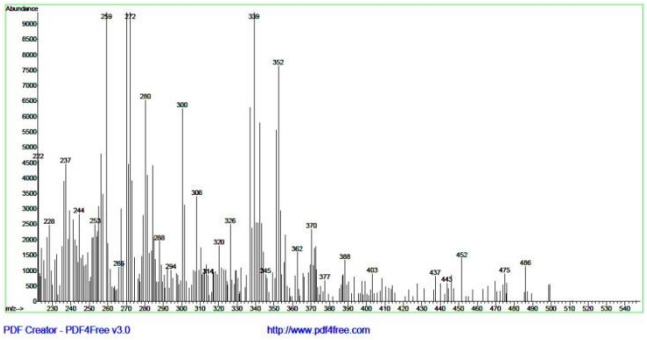

Fig. 3. Mass spectra of [Cr(L) Cl3]

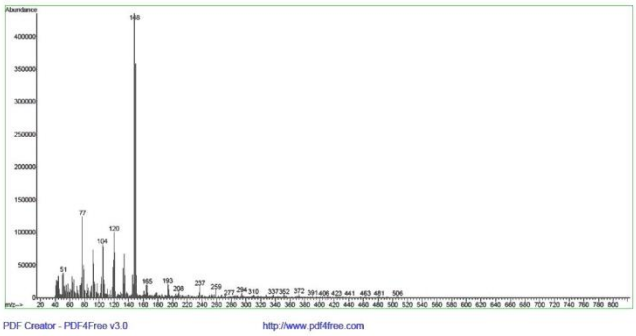

Fig. 4. Mass spectra of [Fe(L) Cl3]

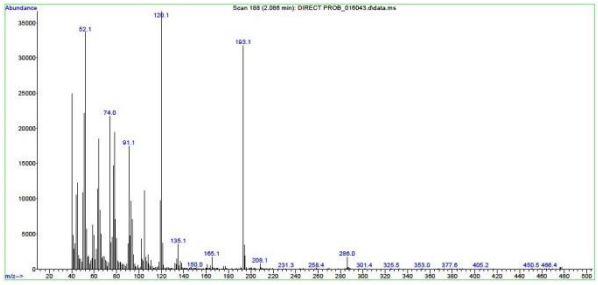

Fig. 5. Mass spectra of [Co(L)Cl2]

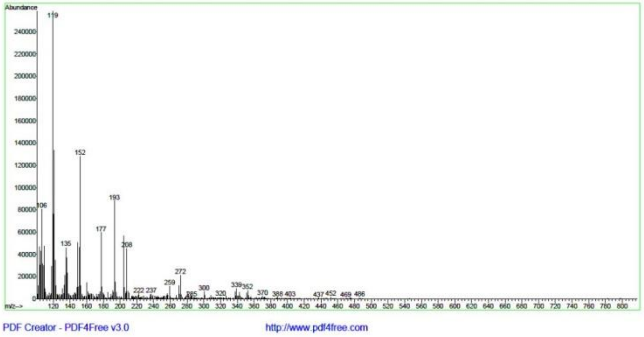

Fig. 6. Mass spectra of [Ni(L)Cl2]

C. Optical Properties

Figure (7) shows the optical absorbance curve versus wavelength with a range of (200-900) nm at room temperature for ligand and its complexes thin films. There is one peak that can be seen for pure ligand at 323 nm related to π-π*, while there are two peaks that can be observed for the complexes, one at about 330-345 nm related to π-π* and the other at around 540-567 nm, but they are shifted towards higher wavelengths (red shift). There are evident that the increase in the absorbance (hyperchromic effect) clarified in all spectra of the complexes attributed to the complexation behavior of ligand towards metal ions, confirming the coordination of the ligands to the metallic ions.

Figure (8) shows a plot of absorption coefficient versus photon energy for ligand and its complexes. The absorption coefficient of film was calculated after correction for the reflection losses according to Equation (2). The value of the absorption coefficient plays an important role to the limitation of the type of transition. It is obvious from the same figure that the value of (α) is lower than 104 cm-1 indicating that the transition was an indirect electron transmission.

According to Equation (2), the plots of (αhυ)1/2 versus photon energy are shown in Figure (9) . The lower energy line corresponds to the phonon absorption processes, while the photon energy intercepts at (Eg+Ep). The other corresponds to the phonon emission processes and photon energy intercept at (Eg-Ep).

The energy gap of the ligand films decreases in the order L> Ni (II)/L > Fe(III)/ L> Co(II)/ L and > Cr(III/L) when the ionic radii decrease the values of indirect band gap energy (Eg) and the phonon energy (Ep) are tabulated in Table (2).

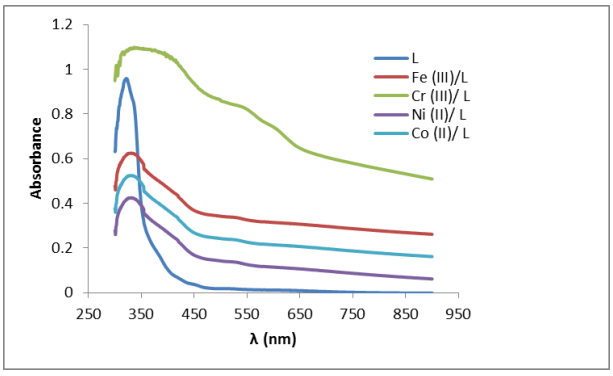

Fig. 7. The relationship between absorption and wavelength for L and its complexes.

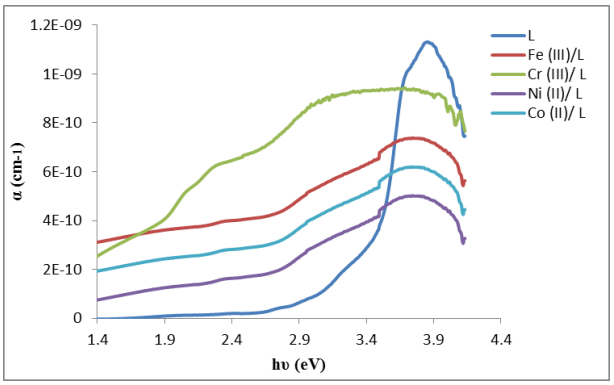

Fig. 8. The relationship between absorption coefficient and photon energy for L and its complexes.

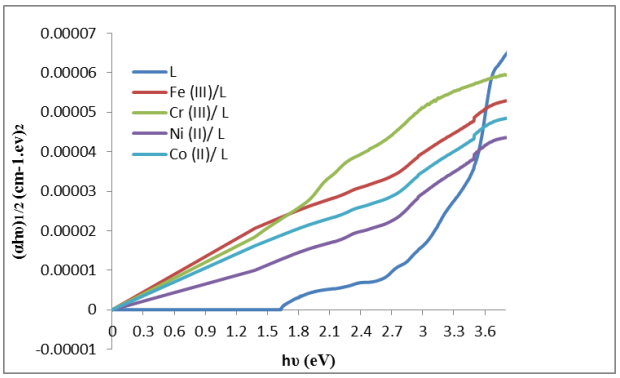

Fig. 9. The relationship between (αhυ)1/2and photon energy for L and its complexes.

TABLE 2. Indirect band gap energy (Eg) and the phonon energy (Ep) values for compound and its complexes

compound	E_g^{ind}	E_p
L	2.85	1.1
Cr	1.15	0.45
Fe	1.5	0.7
Co	1.3	0.6
Ni	1.9	0.9

Figures (10) and (11) show the relationship between real part (ε_r) and imaginary part (ε_i) of dielectric constant with photon energy for ligand and its complexes. The real and imaginary parts were computed from Equations (7) and (8), respectively. The real part is associated with how much it will slow down the speed of light in the material and the imaginary part illustrates that how a dielectric constant absorbs energy from electric field due to dipole motion. It is clearly obvious, for (ε_r) that the value decreases, and (ε_i) increase in the order of decrease of ionic radii as follows: Ni> Fe > Co >Cr [13].

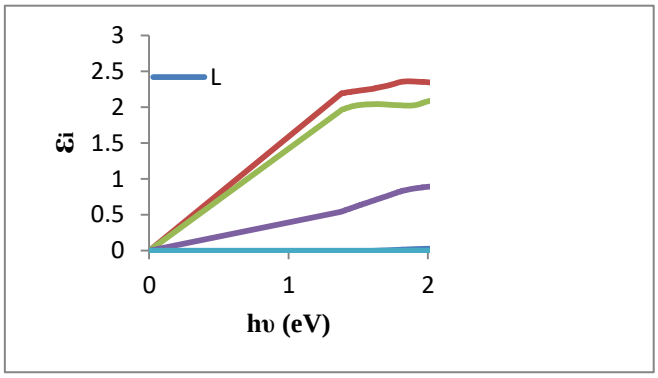

Fig. 10. The relationship between real part and photon energy for L and its complexes.

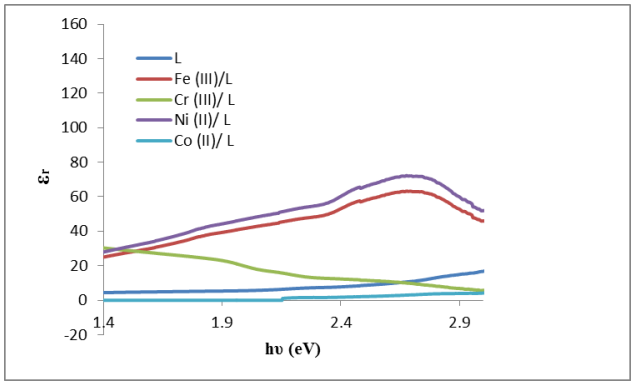

Fig. 11. The relationship between imaginary part and photon energy for L and its complexes.

Figure (12) shows the relationship between optical conductivity and photon energy for ligand and its complexes. The optical conductivity was determined using equation (9). It is clear that there is an increase in optical conductivity as increasing in the order L < Ni (II)/L < Fe(III)/ L< Co(II)/ L and < Cr(III)/L . The increase in optical conductivity is due to the high absorbance of ligand with different transition metals thin film or may be due to electron excited by photon energy. Also, it may be caused by the hopping of the charge carriers between the localized states as well as due to the excitation of the charge carriers to the states in the conduction band [Doering. et .al .2006 , Dharkar. et .al .2012].

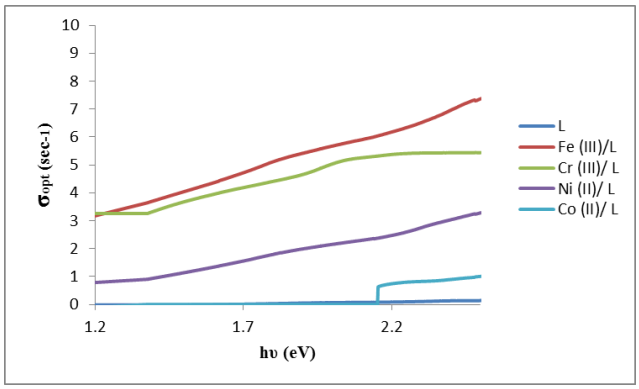

Fig. 12. The relationship between optical conductivity and photon energy for L and its complexes.

IV. CONCLUSION

The ligand 3-(5-(2-(2,3-dimethoxybenzylidene) hydrazinyl) 1,3,4-oxadiazol-2-yl]phenol was successfully synthesized. The FTIR, Mass spectra observations suggest the octahedral geometry for the Cr(III), Fe(III) and tetrahedral geometry was proposed for Co(II) while square planar geometry for Ni (II). The optical transmission spectrum is used to calculate the optical Parameters such as absorption coefficient, imaginary part and optical conductivity where found to be increase, while the energy gap and real parts decrease in the order of decrease of ionic radii as follows Ni> Fe > Co >Cr.

V. REFERENCES

Athraa, H.M.; Zainab AA. M.and Sanaa, M.A. (2012). Synthesis and biological activity of monocyclic Spiro Azetidine-2- one. Journal of College of Education for Pure Science, 2 (1):67-74.

Athraa, H.M.; Asaad, H.S. and Hayder, J.A. (2019). Synthesis, antioxidant activity of some novel schiff base derived from ethyl 4- aminobenzoate. Biochem. Cell. Arch. , 19(1) : 1247-1256.

Athraa, H.M. and Sajda M.T. (2019). Synthesis, characterisation and antibacterial evaluation of some novel 1- phenyl-1h-tetrazole-5-thiol derivatives. International Journal of Research in Pharmaceutical Sciences, 10(2):1136-1142.

Doering, H. (2006). High resolution length sensing using PMMA optical fibres and DDS technology. In: Proc. 15th Int. Conf. on Plastic Optical Fibers,: 238–241.

Dharkar, K.P.; Ingle S.S. and Kalambe A.B. (2011). Electrical Conductivity Properties of Newly Synthesized Melamine - Aniline - Formaldehyde Terpolymer and its Polychelates ,E-Journal of Chemistry8(1): 127-130.

Ezema, F.I. (2005). Optical Characterization of Chemical Bath Deposited Bismuth Oxyiodide (BiOI) Thin Films. Turk J. PHYS, 29: 105-114.

Farhanullah, D.; Tripathi B.K.; Srivastava A.K. and Ram V.J. (2004). Synthesis and glucose-6-phosphatase inhibitory activity of (thiouriedo)alkanoic acid esters. Bio. Med. Chem. Lett., 14(10): 2571-2574

Hussein, N.N.; Asim A.B.; Ghaleb, A.W. and Ahmed, K.K. (2014). Study of the Optical Properties of Poly (Methyl Methaacrylate) (PMMA) Doped with a new Diarylethen Compound. Academic Research International, 5(1): 48-56.

Ibrahim, A.F. and Samah, H.K. (2012). Synthesis and Chracterization of 1,3,4- oxadiazole derivatives with some new transition metal complexes, J. kerbala university ,10(3): 197-209.

Khan, B.T.; Najmuddin, K.; Shamsuddin, S. and Zakeeruddin, S.M. (1990). Mixed ligand complexes of cis-dichloroethionine palladium(II) with purines, pyrimidines and nucleosides. Inorg. Chim. Acta,170 (1):129-131.

Khan, B.T.; Venkatasubramanian, K.; Najmuddin, K.; Shamsuddin, S. and Zakeeruddin S.M. (1991) . Crystal and molecular structure of cis-dichloroethionineplatinum(II) and its interaction with adenine, hypoxanthine, cytosine and their nucleosides. Inorg. Chim. Acta, 179(1): 117-123..

Kushwaha, A.D.; Hiwase, V.V. and Kalambe A.B.,(2012). Electrical Conducting Behaviour of Newly Synthesised p-Nitrophenol-Resorcinol-Formaldehyde Terpolyligand and its Polychelates, European Journal of Applied Engineering and Scientific Research, 1 (2):57-60 .

Redha, I.H.; Mazin, J.H and Athraa, H.M. (2015) Synthesis and Characterization of New Saccharin Derivatives. Int. J. of Multidisciplinary and Current Research, 2015 , 3 (1) : 61-72 .

Redha, I.H.; Mazin, J.H and Athraa, H.M. (2014). Synthesis of Novel Compounds Derived from Saccharin. International Journal of Science and Technology, 3(9): 521-533.

Sheats, J.E.; Hessel, F.; Tsarouhas, L.; Podejko, K.G.; Porter, T.; Kool, L.R. and Nolen, R.L. (1984). Synthesis of Organometallic Polymers for Inertial Fusion Applications. New Monomers and Polymers, Plenum Press, New York. 269-284.

Saddam, H. M.; Zakaria, C.M. and Zaman, B. (2017). Synthesis, Spectral and Thermal Characterization of Cu(II) Complexes with Two New Schiff Base Ligand towards Potential Biological Application, Der Chemica Sinica, 8(3):380-392

Samah, H.K. (2012).Transition metal complexes with tridentate ligand 1E,2E - ethanedial (2,4-dinitro phenyl) hydrazone [5-(2-hydroxyphenyl)-1,3,4-oxadiazol-2-yl]hydrazone J.Thi-Qar Sci.,3(3): 76-87.

Wathiq, S.A.; Huda, M.H. and Athraa, H.M. (2012). Ab initio calculations and structure of three acyclic bis (acetyl acetone)imine derivatives. J. Thi-Qar Sci, 3 (3):149-157

Zoulikha, K.; Adil, A.O. and Bettache, G. (2007). S. Afr.J. Chem., Synthesis and Antibacterial Activity of 1,3,4-Oxadiazole and 1,2,4-Triazole Derivatives of Salicylic Acid and its Synthetic Intermediates.60:20-24.

Zhu, W.C. and Tang, C.A. (2006). Numerical simulation of Brazilian disk rock failure under static and dynamic loading. Int J Rock Mech Min Sci., 43:236–252.